Nuclear
Instruments and
Methods

Hybrid active pixel sensors in infrared astronomy

Gert Finger,[a*] Reinhold J. Dorn,[a] Manfred Meyer,[a] Leander Mehrgan,[a] Jörg Stegmeier,[a] Alan Moorwood[a]

[a]*European Southern Observatory,Karl Schwarzschild str 2, D-85458 Garching, Germany*

Elsevier use only: Received date here; revised date here; accepted date here

Abstract

Infrared astronomy is currently benefiting from three main technologies providing high performance hybrid active pixel sensors. In the near infrared from 1 to 5 μm two technologies, both aiming for buttable 2Kx2K mosaics, are competing, namely InSb and HgCdTe grown by LPE or MBE on Al_2O_3, Si or CdZnTe substrates. Blocked impurity band Si:As arrays cover the mid infrared spectral range from 8 to 28 μm. Adaptive optics combined with multiple integral field units feeding high resolution spectrographs drive the requirements for the array format of infrared sensors used at ground-based infrared observatories. The pixel performance is now approaching fundamental limits. In view of this development a detection limit for the photon flux of the ideal detector will be derived, depending only on the temperature and the impedance of the detector. It will be shown that this limit is approximated by state of the art infrared arrays for long on-chip integrations. Different detector materials are compared and strategies to populate large focal planes are discussed. The need for the development of small-format low noise sensors for adaptive optics and interferometry will be pointed out.

Keywords: Infrared detector, astronomy, sampling technique, HgCdTe, InSb, Si:As, readout noise, dark current, 2Kx2K, wavefront sensor

1. Introduction

Photovoltaic infrared detectors for ground-based astronomical applications have experienced dramatic improvements during the last two decades. The array format has been increased and the pixel performance has improved. With respect to maturity and sensitivity, infrared focal plane technology is catching up with the performance of optical sensors which are still dominated by CCD's for most scientific applications[1].

Infrared detectors exhibit some fundamental differences in the construction of the sensor. Since the band-gap of Silicon is 1.1 eV the sensitivity range of monolithic Silicon CCD's is limited to wavelengths $\lambda<1\mu m$. For longer wavelengths semiconductor materials have to be selected which have a smaller band-gap than the energy of infrared photons. This is the condition for intrinsic photon detection with electrons making a transition from the valence to the conduction band. Two materials, III-V

* Gert Finger. Tel: +49-89-32006256; email: gfinger@eso.org

compounds such as InSb or InGaAs and II-VI compounds such as HgCdTe, are in use. The width of the band-gap of the alloy $Hg_{(1-x)}Cd_xTe$ can be tuned by varying the composition x of the alloy [2]. In this way the sensitivity range and the cut-off wavelength λ_c of the sensor can be matched to the specific application.

In the mid-infrared at wavelengths between 8 and 28 μm blocked impurity band Si:As detectors are used. In these extrinsic Si detectors the absorbed photons generate transitions form the donor level to the conduction band. To increase the quantum efficiency the detectors are heavily doped. The resulting impurity band dark current from D^+ charge transport is eliminated by an undoped blocking layer [3].

2. Hybrid Technology

The readout circuit is realized in Silicon. In most cases the Si multiplexer is a FET-switched CMOS array with a buffer source follower and a reset switch in the unit cell of each pixel. The electrical interconnections between the infrared diodes and the Si multiplexer are made by indium bumps. This hybrid approach makes it possible to optimize the infrared array and the readout circuit separately. Figure 1 shows a cross-section of a HgCdTe detector grown on a sapphire substrate (PACE material) [4].

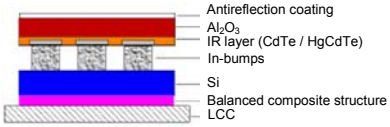

Fig. 1. Cross section of LPE grown HgCdTe active hybrid pixel sensors. The infrared sensitive HgCdTe diode array on a sapphire substrate is bump-bonded to Silicon CMOS readout multiplexer. The thermal mismatch between the Si readout and infrared array is compensated by balanced composite structure.

Increasing the format of hybrid active pixel sensors involves two major challenges. First, the mating force which has to be applied to the hybrid components to produce a robust indium interconnect bond scales with the detector format. Second, when hybrids employing intrinsic narrow bandgap materials are cooled to cryogenic temperatures, they have to cope with the thermal mismatch between the infrared active material, the detector substrate and the Si readout multiplexer, which all have different coefficients of thermal expansion (CTE). The difference in thermal expansion between the detector and the silicon multiplexer has the potential to create large thermally induced stresses on the indium interconnections and the detector material. With repeated thermal cycling this can result in failure of the interconnections, or even lead to damage to the detector pixels.

For HgCdTe arrays, a Balanced Composite Structure (BCS) design has been developed to produce reliable hybrids of detector formats as large as 2Kx2K. This design relieves the stress at the hybrid interface by means of a laminar compressive structure, which is attached to the back side of the mux to match the thermal expansion of the detector material. The thickness and composition of the compressive layer is adjusted to produce the desired compression of the multiplexer. A balancing layer below the compressing layer prevents bending of the FPA.

InSb arrays are thinned by diamond turning. In this case the InSb is made sufficiently thin to follow the thermal expansion of the Silicon multiplexer.

3. Fundamental Performance limits of Photovoltaic detectors operating in CDM

In view of the performance improvements achieved with large format photovoltaic IR detector arrays it is useful to review the operating principle and the fundamental performance limit of photovoltaic detectors operating in the capacitive discharge mode (CDM). The absorbed photon excites an electron from the valence band to the conduction band. If the free electron-hole pair is created within a distance of the pn-junction equal to the diffusion length of the minority carriers it is separated by the electric field of the junction. A reset switch connects the diode to the external bias voltage. After this switch is opened the detector junction is floating. Each absorbed photon discharges the capacity by one electron. The integrating node capacity C is the

combined capacity of the detector and the gate of the source follower in the unit cell of each pixel. The integration ramp is sampled at the beginning and at the end of the exposure. From the variance of the voltage difference $\langle \Delta V^2 \rangle$ the readout noise $\langle \Delta N_{rms} \rangle$ expressed in electrons can be derived as given by the equation EQ1 [5]:

$$\Delta N_{rms}(\tau) = \sqrt{\frac{2KTC}{q^2}\left(1 - e^{-\frac{\tau}{\tau_C}}\right)} \qquad (EQ1)$$

$\tau_c = RC$ is the autocorrelation time corresponding to the diode impedance R and the sensing node capacity C of the integrating node. τ is the time interval between the two voltage readings.

Assuming typical parameters for state-of-the-art detectors e.g. C= 40 fF, dark current of 0.1 e/sec at 1 V reverse bias, the correlation time τ_C=2.5 10^6 sec. In practice, the two voltage readings are completely correlated with $\tau << \tau_C$, and equation (EQ 2) is reduced to $1/q\sqrt{2KT\tau/R}$ yielding 1.1 e rms for an integration time of τ =900 sec. The photon shot noise of photon flux Φ_{phot} is equal to $\sqrt{\Phi_{phot}}$. If the smallest detectable photon flux Φ_{limit} is defined to have an associated photon shot noise equal to the correlated case of equation (EQ 1) we obtain:

$$\Phi_{\text{limit}} = \frac{2KT}{q^2 R} \qquad (EQ2)$$

In the ideal case of a noise-free detector multiplexer and acquisition system, the smallest detectable photon flux Φ_{limit} is proportional to the detector temperature T and inversely proportional to the detector impedance R and becomes independent of the integration time τ. With the parameters assumed above, the limiting flux is 2.2 photons/hour. With multiple sampling the HAWAII array achieves read noise values of 3 e rms. This is of the same order of magnitude as the fundamental noise limit derived in equation (EQ 2) for the correlated case and long integration times [8].

The pixel transfer function which gives the signal in Volts per electron is inversely proportional to the pixel capacity. In order to reduce the read noise, the capacity of the detector must be as small as possible. However, in many applications the detector has to handle the high flux levels of the thermal infrared as well. The available read-out time depends on the full well of the detector and is proportional to the pixel capacity. In order to reduce the required read speed for thermal broad band imaging, a trade-off between full well capacity and readout noise must be considered. Furthermore, limits are imposed on reducing the size of the unit cell FET since smaller FET's tend to have increased 1/f noise.

4. Comparison of detector materials

In the spectral range from λ=1 to 5 μm two detector materials, InSb and HgCdTe are competing to serve both ground and space-based astronomical applications. InSb is the simpler compound and has been used widely for applications including the L and M band atmospheric windows. Because of the long cut-off wavelength of λ_c=5.2 μm InSb detectors have to be cooled down to an operating temperature of 30K. The attractive feature of $Hg_{(1-x)}Cd_xTe$ is the tuneability of the cut-off wavelength which can be set to 2.5 μm to cover the spectral range of near infrared instruments up to the K-band. Mostly HdCdTe arrays grown by liquid phase epitaxy (LPE) on a sapphire substrate, the so-called PACE process, have been used. Photovoltaic n-on-p diodes are formed by implanting boron ions in the p-type substrate [4]. PACE arrays are widely spread and have achieved excellent performance at operating temperatures between 60 and 80 K [10].

Recently, more advanced detector technologies have become available for the manufacture of HgCdTe arrays. The LPE process can now be replaced by molecular beam epitaxy (MBE). The HgCdTe diode array consists of a double layer planar heterostructure (DLPH) grown on a CdZnTe substrate [6]. The crystal lattice of the substrate is better matched to HgCdTe, which results in much lower dislocation and void defect densities. Contrary to the PACE material, the DLPH MBE diodes are produced by a p-on-n heterostructure process. The surface or capping layer is formed by a wider band gap material than the narrow band-gap HgCdTe infrared absorbing layer. The p-type side of the diode is produced by As implantation through the capping layer into the n-type base material. A cross section of the diode structure is shown in Figure 1. The

* Gert Finger. Tel: +49-89-32006256; email: gfinger@eso.org

outcome of this fabrication process is an HgCdTe array with near-theoretical performance.

The performance of different detector materials having different cut-off wavelengths is compared in Figure 3, where the dark current density is plotted against temperature. InSb is represented by triangles, HgCdTe grown by LPE by circles, and HgCdTe grown by MBE is represented by squares. Clearly, MBE grown HgCdTe with λ_c=5μm outperforms InSb at temperatures above 60K [5,6,7,8].

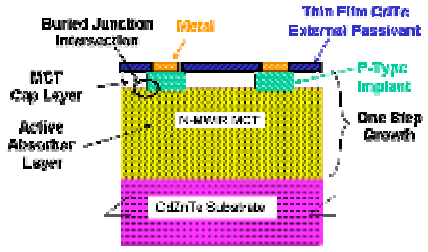

Figure 2. Detector cross section of p-on-n Double Layer Planar Heterostructure photodiode array grown by molecular beam epitaxy

The dark current density for MBE-grown HgCdTe is 5 orders of magnitude lower than for InSb. Due to the fortuitous lattice match of HgCdTe and CdZnTe, defect and dislocation densities are very low. Since the diode junction is not located close to the surface but buried in the bulk of the detector material, it achieves diffusion-limited theoretical performance down to operating temperatures of 60K. The diffusion-limited detector dark current of MBE grown HgCdTe is proportional to $\exp(-E_g/kT)$, whereas the dark current of InSb and LPE grown HgCdTe is dominated by a surface current generation-recombination process, which exhibits a temperature dependence proportional to $\exp(-E_g/2kT)$. Diffusion-limited performance of 5 micron cut-off MBE grown HgCdTe is a major breakthrough in detector technology.

For λ_c=2.5 μm the detector dark current of MBE HgCdTe relative to LPE HgCdTe is reduced by more than 3 orders of magnitude at a specific operating temperature. Measurements performed with MBE grown 256x256 PICNIC arrays with a cut-off wavelength of λ_c=1.7μm are also included in Figure 2. At an operating temperature of 100K this material is not diffusion-limited. If the detectors can be cooled down to temperatures as low as 30K, the generation-recombination process of InSb is frozen out and the dark current of both InSb and MBE grown HgCdTe arrays is dominated by tunnel and surface leakage currents which no longer exhibit a strong temperature dependence. In this temperature regime the performance of the two detector materials is comparable [7][8].

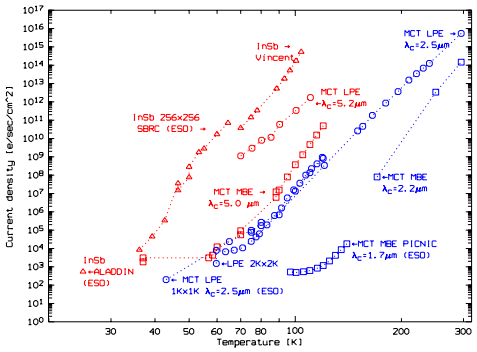

Figure 3. Comparison of dark current for different detector materials: Triangles: InSb. Circles: Liquid phase grown HgCdTe. Squares: Molecular beam epitaxy grown HgCdTe. Both LPE and MBE HgCdTe have different cut-off wavelengths λ_c. MBE grown HgCdTe with λ_c=5 μm (red) comparable to LPE grown HgCdTe withλ_c=2.5μm (blue).

The quantum efficiency of InSb is close to 0.9 over the whole sensitive spectral range of the detector while LPE grown HgCdTe generally has a somewhat lower quantum efficiency than InSb at short wavelengths around λ=1.1 μm. The quantum efficiency of LPE HgCdTe is in the range of 0.65 to 0.7 [9][10].

Because of their low defect densities, MBE-grown HgCdTe arrays have negligible persistence. This has been demonstrated on a 256x256 HgCdTe PICNIC array which has a cut-off wavelength of λ_c=1.7 μm [10].

5. Format and packaging of IR arrays

There are different ways to fill a large focal plane with detector pixels. The first approach simply relies on the fast advances of semiconductor technology of both silicon and III-V compounds as well as II-VI alloys, which will provide larger array formats. Within the last decade the number of pixels of single arrays has increased by more than one order of magnitude and has arrived at formats as large as 2Kx2K [9][11]. The size of available detector substrates will eventually impose a limit on the format of detectors. InSb wafers of 100 mm currently limit the format to 2Kx2K. However, 150 mm InSb substrates are under development, making 4Kx4K arrays feasible in the future [9]. Presently, CdZnTe substrates with 60 mm diameter limit the format of HgCdTe arrays to 2Kx2K. Alternative substrates for HgCdTe such as Si and Al_2O_3 constitute a viable approach to larger formats, but limit the pixel performance because of higher dislocation densities due to the imperfect lattice match of the detector material and the substrate.

The largest IR focal plane currently under development are the arrays for the Infra-Red Survey Telescope VISTA which is being built by the UKATC for the ESO VLT [12][13].VISTA is a wide field telescope which has a diameter of 4 meters. It will be dedicated to IR imaging surveys. The focal plane is located in the Cassegrain focus and will be populated with 16 2Kx2K science detectors packed at 90 % spacing. The VIRGO detector produced by Raytheon has been selected for VISTA. It is a LPE HgCdTe array grown on a CdZnTe substrate. The pixel size is 20 μm. Each detector has 16 parallel outputs organized in parallel stripes, which can be read at a pixel rate of 400 KHz. The total channel count adds up to 256 channels. The scaleable ESO controller IRACE will be used to read out the complete VISTA focal at a frame rate of up to 1.6 Hz.

The ORION array from Raytheon shown in Figure 8 is the first 2Kx2K InSb array. The package of the array is two-side buttable to make a mosaic of four arrays [14]. The ORION array has 64 parallel outputs organized in stripes which can be read at frame rates of 10 Hz. The Orion array was selected to fill the focal plane of the NOAO 4Kx4K 1-2.5 μm IR Imager NEWFIRM providing a field-of-view of approximately 30 arcminutes square with a pixel scale of 0.4 arcsec [15].

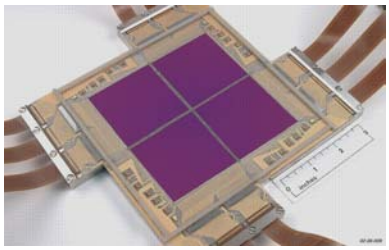

Figure 4. Orion 4x2Kx2K InSb array mosaic package

Another example of a 3 side close buttable 2Kx2K array is the Hawaii-2RG which was selected to equip the 4Kx4K focal plane of the near infrared camera on JWST, an 8-meter space-based telescope, to be positioned at Lagrangian point L2. The Hawaii-2RG multiplexer has 32 outputs which are organized in parallel stripes. A unique feature of the Hawaii-2RG is the guide mode. A guide window of arbitrary size and location can be read out in an interleaved way with the full science frame. The package of the 4Kx4K mosaic for the JWST consisting of four Hawaii-2RG detectors is shown in Figure 5.

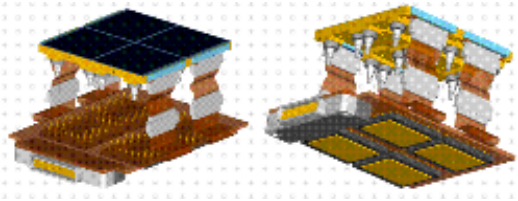

Figure 5. Hawaii-2RG 4x2Kx2K HgCdTe mosaic for the NGST. ASIC's below detectors for clock and bias generation as well as analog to digital conversion of video signal. Electrical connection between ASIC's and arrays by flexible boards.

Each of the four arrays is connected by a flexible board to an application-specific integrated circuit (ASIC), which integrates a complete detector

* Gert Finger. Tel: +49-89-32006256; email: gfinger@eso.org

controller including freely programmable clock and bias generation as well as 16 bit analog to digital conversion of all 32 outputs of the Hawaii2RG on a single ASIC chip [16]. The only communication of the ASIC to the outside world is through a LVD or CMOS digital bus. Since the high impedance low level video signal of the detector no longer has to be transmitted over a long cable to the ADC of the external controller, but is digitized immediately on the focal plane, a lot of the "black magic" used to obtain good noise performance is eliminated. Presently, the first ASIC's have been fabricated and are being tested.

6. Sensors for adaptive optics and interferometry

At present the infrared wavefront sensor installed in the ESO VLT adaptive optics system NAOS utilizes one quadrant of a Hawaii 1Kx1K array.[18]. This AO system using a Shack-Hartmann sensor delivers diffraction limited images for the science instrument CONICA, which is equipped with an Aladdin 1Kx1K InSb array [17]. First results obtained with the IR wavefront sensor in the K-band achieved a Strehl ratio of ~ 0.55. The goal is to increase the Strehl ratio to 0.7 with an AO optimized system.

The ESO VLT interferometer (VLTI) initially obtained first fringes by combining light from two siderostats and later by combining two 8-meter telescopes. The VLTI commissioning instrument VINCI also utilizes one quadrant of a Hawaii 1Kx1K array which has to acquire the intensity of four spots at a rate of >1KHz to cope with the effects of atmospheric turbulence [19]. A fringe tracker FINITO is being built to stabilize the fringes and allow for long integrations with the science instruments [20]. If the beams of three telescopes are combined, this fringe tracker utilizes only seven pixels of the PICNIC 256x256 HgCdTe array, four pixels for the interferometric fiber outputs and three pixels for the photometric fiber outputs, which are imaged onto the detector as shown in Figure 6. For the two illuminated pixels in each quadrant, exactly the same positions are used to benefit from the multiplex advantage by always reading out four pixels simultaneously.

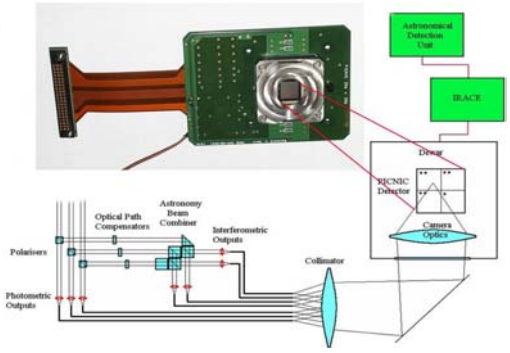

Figure 6. Layout of fringe-tracker FINITO with the combination of three telescopes.

Both AO sensors and fringe-trackers have integration times well below 1 ms. The readout noise of 10 to 20 e rms severely limits their performance, especially at shorter wavelengths with reduced thermal background.

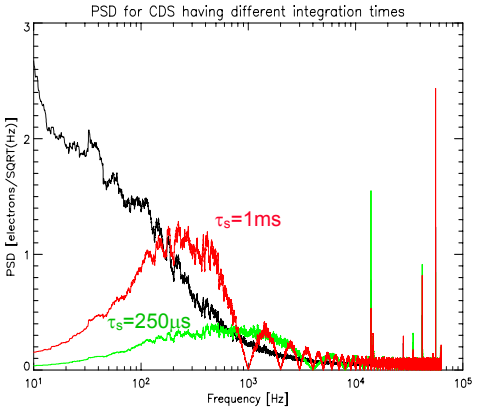

Figure 7. Power spectral density (PSD) of video output taken with 256x256 MBE PICNIC λ_c=1.9 μm array. Upper curve: raw spectrum. Middle curve: PSD for double correlated clamp (DCS) and integration time of 1ms. Lower curve: PSD for DCS and integration time of 250 μs.

In Figure 7 the power spectral density of the video output measured with the λ_c=1.9 μm PICNIC

256x256 MBE array is shown. Most of the power spectral density (18 e rms) is contained at low frequencies below 1 KHz. The total noise is 32 e rms. The power spectrum multiplied by the transfer function [2-cos($2\pi f\tau_s$)] of a double correlated clamp is also shown for integration times of τ_s =1 ms and τ_s =250μs. For short integration times double correlated sampling removes a major part of the low frequency noise, resulting in a total readout noise of 14 e rms.

Clearly, further development is needed. A multiplexer having 256x256 pixels, a capacitive trans-impedance amplifier in the unit cell, 32 parallel outputs, a frame rate of > 1 KHz and a readout noise of ~ 1 e rms has to be envisaged. At Rockwell a prototype AO multiplexer with 7 different readout architectures is under development.

7. Conclusions

Both InSb and HgCdTe arrays with formats as large as 2Kx2K have come on-line. Diffusion limited performance has been achieved down to temperatures of 60 K with MBE-grown HgCdTe double-layer planar heterostructures. The arrays are packaged in buttable mounts which facilitate the construction of large mosaics needed to equip next generation instruments. The development of an application-specific integrated circuit for the Hawaii-2RG array will allow control of the array and digitizing the detector signal directly on the focal plane. The ASIC may eventually replace the conventional detector controller. There is a clear need to develop a specialized small format, high-speed low-noise detector for adaptive optics systems and IR sensors used in active control loops.

References

[1] J. Janesick, SPIE oe magazine, pp 30-33,Feb 2002.

[2] . D. Long and J. L. Schmit, vol.5, Semiconductors and Semimetals, Infrared Detectors, edited by R. K. Willardson and A. C. Beer, Academic Press, New York, pp. 175, 1970

[3] Petroff and M.G. Stapelbroek, *Blocked impurity band detectors*, U.S. Patent No. 4568960, February 4, 1986.

[4] C.A. Cabelli, D.E. Cooper, A. Haas, L.J. Kozlowski, G. Bostrup, A.C. Chen, J.D. Blackwell, J.T. Montroy, K. Vural, W. E. Kleinhans, K.W. Hodapp, D.Hall, Proc. SPIE vol. 4028, pp. 331-342, 2000.

[5] G. Finger, G. Nicolini, M. Meyer, A.F. M. Moorwood, Proc. SPIE vol. 2475, pp. 15-26, 1995.

[6] R Bailey, J. Arias,W. McLevige, J. Pasko, A. Chen, C. Cabelli, L. Kozlowski, K. Vural, J. Wu, W. Forrest, J. Pipher, Proc. SPIE vol. 3354, pp. 77-86, 1998.

[7] D. Hall, , "The University of Hawaii / Rockwell Scientific Program to develop MBE HgCdTe based NIR Mosaic FPA for NGST",Workshop on Scientific Detectors for Astronomy, 2002, to be published.

[8] G. Finger, H. Mehrgan, M. Meyer, A. F. M. Moorwood, G. Nicolini and J. Stegmeier, Proc. SPIE vol. 4008, pp 1280-1297, 2000.

[9] K. J. Ando, P. J. Love, N. A. Lum, D. J. Gulbransen, A. W. Hoffman, E. Corrales, R. E. Mills, M. E. Murray, "Overview of Astronomy Arrays at Raytheon Infrared Operations",Workshop on Scientific Detectors for Astronomy, 2002, to be published

[10] G. Finger, R. J. Dorn, H Mehrgan., M. Meyer, A.F. M. Moorwood and J. Stegmeier, Workshop on Scientific Detectors for Astronomy, "Test Results with 2Kx2K MCT arrays", 2002, to be published

[11] L. J. Kozlowski, M. Loose, Y. Bai, J. Luo, S. Xue, G.W. Hughes and K. Vural, "Progress in Ultra-low Noise Hybrid and Monolithic FPAs for Visible and Infrared", Workshop on Scientific Detectors for Astronomy, 2002, to be published.

[12] S. C. Craig and A. McPherson, "VISTA Project Overview", http://www.roe.ac.uk/atc/projects/vista/home_info/overview, 2001.

[13] D. Ives, N. Bezawada and M. Ellis, "Detector Work at the UKATC: From the Optical to the Sub-millimetre", Workshop on Scientific Detectors for Astronomy, 2002, to be published.

[14] A.M. Fowler, M.K. Merrill, W. Ball, A. Hendon, F. Vrba, and C. McCreight,, Proc. SPIE vol. 4841, pp 853-859, 2002.

[15] R. G. Autry, R. G. Probst, K. Abdel-Gawad, National Optical Astronomy Observatory; R. D. Blakley; P. N. Daly, R. Dominguez, E. A. Hileman, M. Liang, E. T. Pearson, R. A. Shaw, D. Tody, Proc. SPIE vol. 4841, pp 525-539, 2002.

[16] M. Loose, L. Lewyn, H. Durmus, J. D. Garnett, D. N. B. Hall, A. B. Joshi, L. J. Kozlowski and I. Ovsiannikov Proc. SPIE vol. 4841, pp 782-794, 2002.

[17] R. Lenzen, M. Hartung W. Brandner, G. Finger, N. N. Hubin, F. Lacombe, A. Lagrange, M. D. Lehnert, A. Moorwood, and D. Mouillet, Proceedings SPIE vol. 4841, pp 860-868, 2002.

[18] E. Gendron, F. Lacombe, D. Rouan, J Charton, C. Collin, B. Lefort, C. Marlot, G. Michet, G. Nicol, S. Pau, V.D. Phan, B. Talureau, J.L. Lizon, N. Hubin, Proc. SPIE vol. 4839, pp 195-205, 2002.

[19] P. Kervella, P. B. Gitton, E. di Folco, T. Duc, M. Kiekebusch, P. Ballester; W. D. Cotton, V. Coude du Foresto, A. Glindemann, A. Longinotti, M. Schoeller, R. Wilhelm and M. Wittkowski, Proc. SPIE vol. 4838, pp 858-869, 2002.

[20] M. Gai, Beyond Conventional Adaptive Optics, Eds. R. Ragazzoni, N. Hubin and S. Esposito, ESO Conference & Wokshop Proceedings 58, pp 329-334, 2001.

* Gert Finger. Tel: +49-89-32006256; email: gfinger@eso.org